Received February 18, 2020, accepted March 4, 2020, date of publication March 12, 2020, date of current version March 24, 2020.

Digital Object Identifier 10.1109/ACCESS.2020.2980250

Analysis of the Singular Values for Conductivity Reconstruction in Magneto-Acoustic Tomography With Magnetic Induction

REN MA, MING YANG, SHUNQI ZHANG, XIAOQING ZHOU, TAO YIN, (Member, IEEE), AND ZHIPENG LIU, (Member, IEEE)

Institute of Biomedical Engineering, Chinese Academy of Medical Sciences and Peking Union Medical College, Tianjin 300192, China

Corresponding authors: Tao Yin (bme500@163.com) and Zhipeng Liu (lzpeng67@163.com)

This work was supported in part by the National Natural Science Foundation of China under Grant 61701545, Grant 81772004, and Grant 81772003, in part by the Key Program of Natural Science Foundation of Tianjin under Grant 17JCZDJC32400, in part by the Natural Science Foundation of Tianjin under Grant 19JCQNJC12900, and in part by the CAMS Initiative for Innovative Medicine under Grant 2017-I2M-3-020.

ABSTRACT Due to the acoustic source distribution and limited bandwidth ultrasound measurement, the dominant ultrasound signals always come from the boundary of the electrical conductivity in magneto-acoustic tomography with magnetic induction (MAT-MI). To make full use of the strong boundary ultrasound signals, a system matrix is built which shows the relationship between the electrical conductivity and the ultrasound signals. By analyzing the singular values of the system matrix, the necessary signal to noise ratio(SNR) level is estimated in this study. An inverse procedure based on the truncated singular value decomposition(TSVD) method is presented to improve the quality of the reconstructed MAT-MI image. Simulation results show that the reconstructed conductivity images by using the new algorithm match better than that of the back-projection algorithm. Both the simulation results and the experiment results prove the reconstructed image is close to the original conductivity distribution when the more singular values are used in the inverse procedure. Meanwhile, as the number of singular values increases, the effect of noise will be enhanced in the reconstructed image. The proposed reconstruction algorithm can improve the quality of the reconstruction image for a low SNR system. Moreover, the system matrix based reconstruction algorithm proposed in this work will help to analyze the physical process and to obtain accurate high-resolution reconstructions for MAT-MI.

INDEX TERMS Magneto acoustic tomography with magnetic induction, singular values decomposition, system matrix, inverse problem, electrical conductivity.

I. INTRODUCTION

Previous studies have shown that the electrical conductivity of biological tissue is an important parameter for disease detection. The electrical conductivity is significantly different in the tissue under different physiological and pathological conditions [1]–[3]. Especially, it can be used to detect cancer which is at a very early stage. Magneto-acoustic tomography with magnetic induction (MAT-MI) [4] is a non-invasive electrical conductivity imaging technology of biological tissues. In a MAT-MI configuration, the magneto-acoustic signals are collected using a certain amount of ultrasound transducers placed around the tissues. The signals are then processed through a reconstruction algorithm, and an image with the conductivity information is generated. The image quality and accuracy of conductivity can be greatly enhanced when a realistic model is built.

In the past several years, several reconstruction algorithms of MAT-MI have been designed. Analytical reconstruction algorithms such as the back-projection algorithm and time reversal method were based on idealized imaging models that assumed a lossless and acoustically homogeneous medium. For obtaining a better image of conductivity, many reconstruction algorithms based on a more actual model were introduced. Xia *et al.* demonstrated the reconstruction algorithm of vectorial acoustic sources. Their results show that the scalar acoustic measurements can be vectorized according to the known measurement geometry under certain conditions [5]. Sun et al considered the acoustic sources as dipole radiation and developed the corresponding reconstruction algorithm [6]. Mariappan and He shows that using the proposed vector source reconstruction algorithm

The associate editor coordinating the review of this manuscript and approving it for publication was Md. Kamrul Hasan.

combined with Helmholtz decomposition of the induced eddy current, the distribution of the conductivity can be estimated [7]. For a more accurate reconstruction, the reconstruction algorithms focused on real conditions of the MAT-MI system were developed. Such as beam-forming algorithm [8], the effects of acoustic heterogeneity [9] and the ultrasound transducer characteristics [10] were all considered into the reconstruction algorithms of MAT-MI. All the models above didn't show the direct relationship between ultrasound signals and the distribution of the conductivity. Usually, in the MAT-MI experiment, the acquired ultrasound signals are acquired by the bandlimited transducers. It is hard to find a relationship between the conductivity distribution and ultrasound signals. This causes the information from ultrasound signals are not fully used by the current models.

To address these problems, a system model to describe the relationship between detected ultrasound signals and the reconstructed conductivity distribution should be build up. System model based algorithms can be used to compensate the loss of information and get information from the signals with lower SNR by incorporating the detectors geometry in model matrix. This concept has been used in the reconstruction of magnetic resonance imaging(MRI) and computed tomography(CT) in order to reduce the radiation dose and the scan time [11], [12]. In addition, it has been used for thermos-acoustic imaging(TAI) and photo-acoustic tomography (PAT) [13], [14].

In this paper, we introduce a simple and accurate system matrix that models MAT-MI wave generation, propagation and acquisition. The singular values of the system matrix are computed in order to improve the quality of the reconstructed MAT-MI image. After going deep into the system matrix, we find the noise level influences the reconstruction results. Using the proposed method, we are able to get a relationship between the distribution of conductivity and ultrasound signals. We also compare its accuracy with well-known models and present reconstruction results on popular phantom images. We compared the performance of the proposed algorithm with the performance of back projection algorithm under different SNR when the same experiment parameters are used. Quantitative and qualitative results indicate that the proposed method can be a proper option when we face a low SNR MAT-MI system.

II. METHOD

A. FORWORD PROGRAM

In MAT-MI, the magnetic field, induced eddy current and acoustic pressure are the functions of time and space, according to the electromechanical coupling mechanism of electrical, magnetic and acoustic fields in biological tissue, the acoustic pressure distribution is expressed by the following wave equation (1) [15]:

$$\nabla^2 p(r,t) - \frac{1}{c_s^2}\frac{\partial^2}{\partial t^2} p(r,t) = \nabla \cdot [J(r,t) \times B_0] \tag{1}$$

Assuming that the ultrasound speed is equal to c_s in the tissue, $p(r,t)$ is the distribution of acoustic pressure field, $J(r,t)$ is the density of induced eddy current, r represents the location in infinite space, and $\nabla \cdot [J(r,t) \times B_0]$ is the acoustic vibration source. According to Green's function method in infinite space [16], the solution of the unbounded acoustic field in the wave equation is given in formula (2):

$$p(r_d,t) = -\frac{1}{4\pi}\int_{\Omega} \mathbf{d}r \nabla \cdot [J(r,t) \times B_0] \frac{\delta(t - |r - r_d|/c_s)}{|r - r_d|} \tag{2}$$

According to the generation mechanism of MAT-MI acoustic source, the acoustic source is essentially acted upon by Lorentz force and produces vibration. The vibration source produced by force is a dipole acoustic source and the dipole acoustic source can be divided into formula (3) based on Ohm's low:

$$\nabla \cdot [J(r,t) \times B_0] = [\nabla\sigma \times E(r,t) + \sigma \nabla \times E(r,t)] \cdot B_0 \tag{3}$$

From equation (3), the acoustic source is composed of $[\nabla\sigma \times E(r,t)] \cdot B_0$ and $[\sigma\nabla \times E(r,t)] \cdot B_0$. The first part $[\nabla\sigma \times E(r,t)] \cdot B_0$ has a higher frequency component which is only produced at the boundary of conductivity distribution. The latter part $[\sigma\nabla \times E(r,t)] \cdot B_0$ is the inner acoustic source which has a lower frequency. Combine the formula (2) and (3), the ultrasound pressure can be expressed by (4):

$$\begin{aligned} p(r_d,t) = & -\frac{1}{4\pi} \\ & \times \int_{\Omega} \mathbf{d}r [\nabla\sigma \times E(r,t) + \sigma\nabla \times E(r,t)] \\ & \cdot B_0 \frac{\delta(t - |r - r_d|/c_s)}{|r - r_d|} \end{aligned} \tag{4}$$

The acoustic pressure signals are detected by the transducers. Different transducers show different characteristics such as the impulse response, the sensitivity, the linearity and the distribution of the acoustic field. The "ideal point detector" assumption could not be satisfied in real conditions. The transmitting response and receiving response of acoustic transducers will vary with the change of the relative direction. When it is at the transmitting state to radiate the acoustic wave in the medium, the distribution of acoustic energy in the space is uneven. Therefore, the forward problem simulation process of MAT-MI acoustic field requires the establishment of an acoustic transducer model. If the acoustic field distribution function is $w_{r_d}(r,t)$ and the impulse response function is $h(t)$, the acoustic pressure forward problem formula (4) based on receiving characteristics of an acoustic transducer can be obtained as follows:

$$\begin{aligned} p(r_d,t) = & -\frac{B_0}{4\pi}\int_{\Omega} \mathbf{d}r [\nabla\sigma \times E(r,t)] w_{r_d}(r,t) \\ & \times \frac{h(t - |r - r_d|/c_s)}{|r - r_d|} \\ & + \int_{\Omega} \mathbf{d}r \sigma \nabla \times E(r,t) w_{r_d}(r,t) \\ & \times \frac{h(t - |r - r_d|/c_s)}{|r - r_d|} \end{aligned} \tag{5}$$

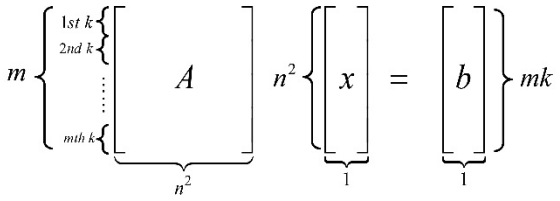

FIGURE 1. The system matrix of MAT-MI.

From equation (5), the collected waveform can be divided into two parts. The second part shows a direct relationship between $\sigma(r)$ and $p(r_d, t)$. Because of the bandwidth limitation of the ultrasound transducer, the first part generating from the boundary of the conductivity is the dominant part of $p(r_d, t)$. This part is produced by the gradient of the electrical conductivity, which can be described by:

$$[\nabla\sigma \times E(r,t)] \cdot B_0 = B_{0z}E_y\frac{\partial\sigma}{\partial x} - B_{0z}E_x\frac{\partial\sigma}{\partial y} \tag{6}$$

The partial differential of $\sigma(r)$ is computed by:

$$\begin{aligned}\frac{\partial\sigma}{\partial x} &= \frac{\sigma(x+dx,y)-\sigma(x,y)}{dx}\\ \frac{\partial\sigma}{\partial y} &= \frac{\sigma(x,y+dy)-\sigma(x,y)}{dy}\end{aligned} \tag{7}$$

where $dx = dy$. Therefore, the equation (6) is described by:

$$\begin{aligned}[\nabla\sigma \times E(r,t)] \cdot B_0 = {} & \frac{B_{0z}E_y}{dx}\sigma(x+dx,y)\\ & -\frac{B_{0z}E_x}{dx}\sigma(x,y+dx)\\ & +(\frac{B_{0z}E_x - B_{0z}E_y}{dx})\sigma(x,y)\end{aligned} \tag{8}$$

Equation (8) shows that, the first part of equation (5) could also make a relationship between $p(r_d, t)$ and σ. This is not only a connection with $\sigma(x, y)$, but also a connection with the neighbor points including $\sigma(x + dx, y)$ and $\sigma(x, y + dx)$.

For a $n \times n$ conductivity reconstruction region, a discrete form of equation (5) could be written by a difference equation as follows:

$$\sum_{y=1}^{n}\Delta y\sum_{x=1}^{n}K(x,y,r_d,t)\sigma(x,y)\Delta x = p(r_d,t) \tag{9}$$

wherein, $K(x, y, r_d, t)$ is the discrete kernel function. By discretization, if the transducer number is set to m and the sampling number of each transducer is set to k, the time dependent series $p(r_d, t)$ could be a matrix of m times k. Then the matrix equation of (9) can be showed by figure 1:

Wherein, $\boldsymbol{A}$ is the system matrix which is the numerical expression of the discrete kernel function $K(x, y, r_d, t)$, $\boldsymbol{x}$ represents the $n \times n$ map of conductivity distribution $\sigma(x, y)$ and $\boldsymbol{b}$ shows the acoustic pressure $p(r_d, t)$ acquired by the ultrasound transducers. To set up the matrix relation equation, $\boldsymbol{x}$ and $\boldsymbol{b}$ are transformed into the column matrix.

B. INVERSE PROGRAM

In the reconstruction process, we model the procedure of MAT-MI using $Ax = b$. The system matrix A means that the contribution of each point of conductivity distribution to the acoustic pressure acquired by an acoustic transducer has a different weight. For a given MAT-MI system, the matrix A is sparse and does not depend on the imaged object, but only on the experimental acquisition geometry. To reconstruct the conductivity image from the measured acoustic signals, the matrix relation equation $Ax = b$ has to be inverted. For this inversion, consider the minimization problem:

$$\arg\min_{x\in\Re^n}\|Ax-b\|_2 \tag{10}$$

where $\|\|_2$ denotes an l_2-norm throughout this paper. As figure 1 shows, A is a matrix with a dimension of $mk \times n^2$, The vector $x \in \Re^{n^2}$ and vector $b \in \Re^{mk}$ are minimization problem (10) with a matrix of this kind often is referred to as discrete ill-posed problems. For notational simplicity, we will assume that $mk \geq n^2$. However, this method discussed also can be applied when $mk < n^2$.

Let A^{-1} denote the pseudo-inverse of A. Because of the noise in MAT-MI measurement system, the solution of equation (10) can be transformed as follows [17]:

$$x = A^{-1}b = A^{-1}b_r + A^{-1}b_n \tag{11}$$

where b_r is the noise free vector of ultrasound signals, b_n is the measurement noise in b. The matrix A means an impulse response of the current system. From equation (11), the reconstruction x is typically dominated by the reconstruction error $A^{-1}b_n$ when A^{-1} has a very large norm. This will cause the conductivity reconstruction distortion or meaningless. The difficulty can be mitigated by replacing the matrix A by a less ill-conditioned nearby matrix. One of the most popular regularization methods for discrete ill-posed problem (10) of small to moderate size is truncated singular value decomposition(TSVD). The system matrix can be expressed as:

$$A = U\Sigma V^* \tag{12}$$

wherein, U and V are orthogonal matrices. The superscript * denotes matrix transposition. Σ is a diagonal matrix which shows the singular values of A, the square roots of the eigenvalues of A^TA are called singular values, where A^T is the conjugate transpose of A. These singular values represent the inherent feature of our MAT-MI measurement system.

$$\Sigma = diag[\sigma_1, \sigma_2, \ldots, \sigma_l], \quad \sigma_1 \geq \sigma_2 \geq \cdots \geq \sigma_l \geq 0 \tag{13}$$

In order to reconstruct the conductivity distribution, we should inverse the system matrix A. The inverse version of equation (12) is given by:

$$A^{-1} = V\Sigma^{-1}U^* \tag{14}$$

wherein, $\Sigma^{-1} = diag[\sigma_1^{-1}, \sigma_2^{-1}, \ldots, \sigma_l^{-1}]$ can be computed for the inverse problems. U and V are orthogonal matrices. The norm of A^{-1} is equal to the norm of Σ^{-1}. For a noise free system, $A^{-1}b_r$ could be reconstructed Because of the noise b_n, the smaller singular values of the system will make $A^{-1}b_n$ larger. Using TSVD method, define the matrix Σ_t by setting the smaller singular values to zero. The matrix is given by:

$$\Sigma_t = diag[\sigma_1, \sigma_2, \ldots, \sigma_t, 0, \ldots, 0] \tag{15}$$

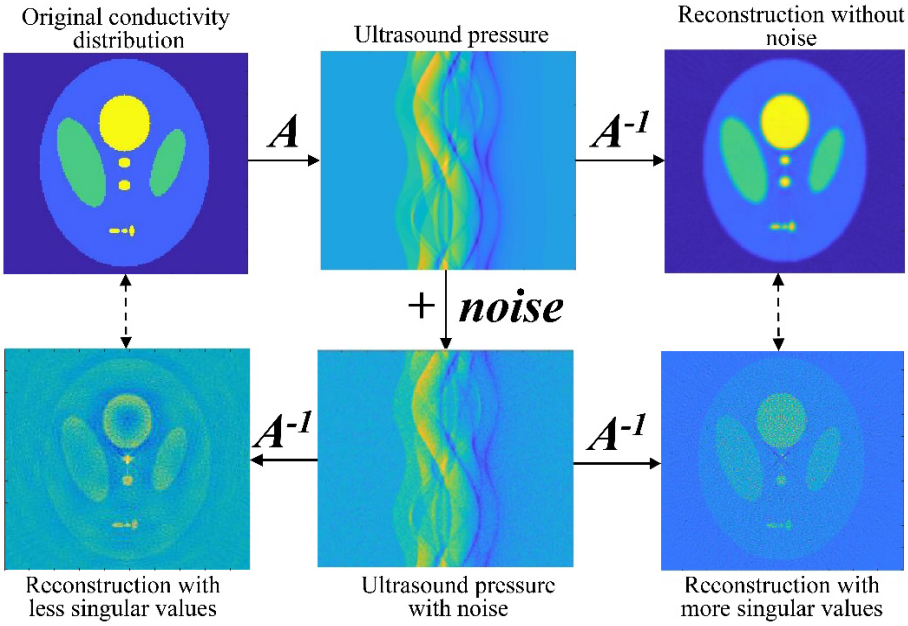

FIGURE 2. The simulation based on system matrix method.

We denote this solution by x_t. It can be expressed with the pseudo-inverse of A_t, which is given by:

$$A_t^{-1} = V\Sigma_t^{-1}U^* \tag{16}$$

Therefore, given a rigid measurement configuration, the system matrix A and its truncated singular values matrix σ_t may be pre-calculated and stored, thus equation (16) can be used for a conductivity image reconstruction.

C. SIMULATION METHODS

In order to verify the effectiveness of the system matrix reconstruction algorithm, a numerical study was performed to analyze the reconstruction scheme considered in this paper. For simplicity, a 2D phantom model of conductivity distribution is established. The conductivity model refers to the commonly used S-L model structure in CT imaging [18], which can carry out performance evaluation on imaging algorithms and simulation experiments. Set the major axis of outer ellipsoids to be 70 mm and its conductivity to be 0.1 s/m, the conductivity of two internal centered big ellipsoids to be 0.2 s/m and conductivity of other internal ellipsoids to be 0.5 s/m. The strength of the static magnetic field B_0 is 1 T. In order to ensure the uniformity of pulse excitation, the excitation magnetic field is generated by Helmholtz coil, the injection current density of this coil is 10^7A.

To reduce the size of system matrix, we restricted our study to a 2D circular-detection geometry. The solution domain is a square of $80mm \times 80mm$, and then it is divided into 201×201 square grids. The scan radius is 72 mm. 200 V303 transducers are used for ultrasound acquisition and the sample number is 500. The simulation is performed as figure 2 shown. The reconstruction was carried out by MATLAB on a homemade workstation.

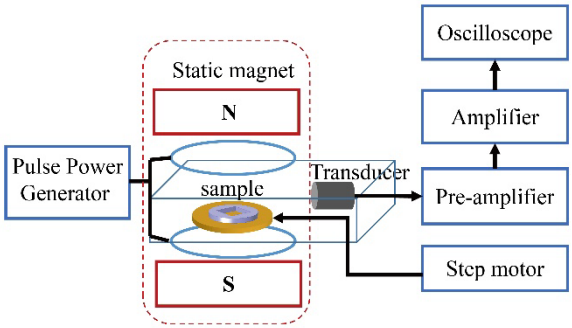

FIGURE 3. Schematic diagram of the MAT-MI experiment.

D. EXPERIMENT SETTINGS

Figure 3 shows the schematic diagram of the MAT-MI experiment. A homemade pulse power generator is used to produce a series of short pulse with the pulse width of 800ns and repetition frequency of 15Hz. The pulsed magnetic field is generated by the electric pulse flowing in the circular coil and its magnetic flux density is approximately 0.008T in the imaging area. The stationary magnetic field is generated by a homemade electromagnet, the maximum magnetic flux intensity is approximately 0.9T. A 13mm-diameter plat transducer (V303, Panametrics) was fastened to a plastic holder and kept facing to the experiment phantom. It had a center frequency of 1MHz and the -3dB bandwidth was from 0.65MHz to 1.2MHz. The ultrasound signals collected by the transducer were amplified with a 40dB low noise amplifier (5072PR, Olympus). In order to improve SNR as much as possible, the conductive silicone rubber with a thickness of 0.51mm (conductivity $\approx$ 8000S/m) is used for the reconstructive phantom. The phantom has a square hole inside a circle. The length of inner square is 20mm and the diameter of the outer circle is 40mm. The phantom is placed in a rotatable platform for a circle scan with a step of 1.8°. The sampling rate is 10 MHz.

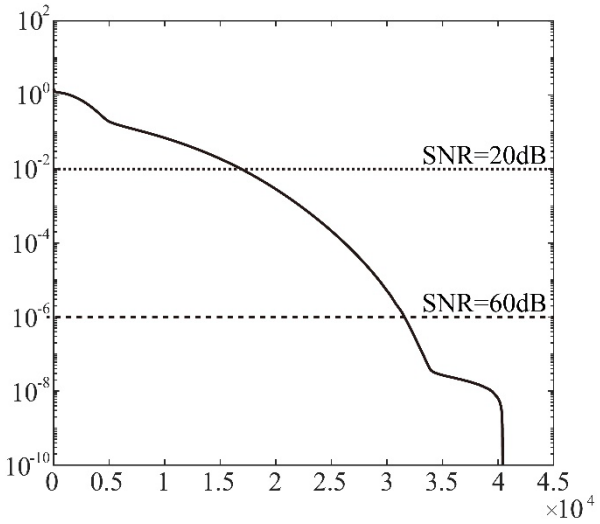

FIGURE 4. The singular values of the system matrix and the relationship between the SNR and the singular values.

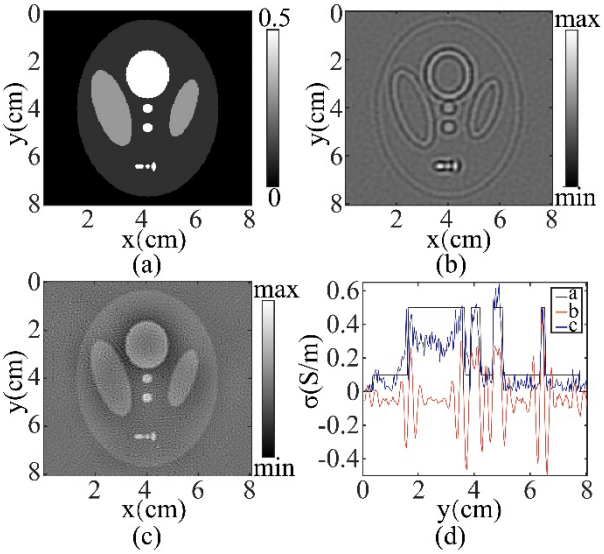

FIGURE 5. Original conductivity distribution and reconstruction results with SNR = 20dB. (a) Original conductivity distribution; (b) reconstruction results using filter back-projection algorithm; (c) reconstruction results using system matrix algorithm;(d) line graph of the conductivity distribution alone x = 4cm in figure (a) to (c).

III. RESULTS

A. SIMULATION RESULTS

There are many approaches described in the literature to determining a suitable truncation index t, including the quasi-optimality criterion, the L-curve, generalized cross validation, extrapolation, and the discrepancy principle. The size of the truncation index t depends on the norm of the error b_n in b. For our system, the size of the system matrix A is 40401 × 100200, it's a sparse matrix. After SVD computation, the system matrix has 40401 eigenvalues, $\sigma_1, \sigma_2, \ldots, \sigma_{40401}$. Figure 4 shows the relationship between the singular values of the current MAT-MI system matrix and SNR. As figure 4 shows, the truncation index has to be chosen smaller to the SNR line. Because the SNR line gives the noise level of our MAT-MI system. The smaller the eigenvalues are, the larger the reconstruction error will be. To avoid severe error in the inverse problem, we choose the SNR line as the truncation index. In the current MAT-MI system, the SNR is about 20dB, so the truncation index is approximately 15000.

To validate our system matrix algorithm, the MAT-MI signals from the phantom are acquired by the forward process with SNR = 20dB. The group of signals are then used for reconstruction. The inverse matrix Σ_t consists of 15000 singular values. The results of the reconstruction are shown in figure 5. Figure 5(a) shows the original conductivity distribution in our simulation experiment. Figure 5(b) shows the reconstructed image using the back-projection algorithm, whereas in figure 5(c) we display the equivalent tomographic image obtained with the system matrix algorithm proposed in this work. The greyscale of the images is set to the normalization. As figure 5(b) shows, only conductivity boundary could be reconstructed by back-projection algorithm because of the transducer characteristics. Figure 5(c) shows that the system matrix algorithm is possible to reconstruct the conductivity distribution, which can be applied to our MAT-MI system. A line graph of the conductivity distribution at x = 4cm was shown in figure 5(d). Compared with the reconstructed image by filter back-projection algorithm, the reconstructed image using the proposed algorithm shows more detailed information.

As a further illustration of the performance of the proposed method, let us consider the number of the singular values we used in the reconstruction. Figures 6(a)-(d) show that the reconstructed images by using different amounts of singular values. The reconstruction obtained with 5000 singular values generally shows more boundary information of conductivity distribution. When the number of the singular values comes to 10000, more detail information of conductivity distribution is reconstructed. Figure 6(c) shows the reconstructed image using 15000 singular values. The reconstructed image achieves good quality, which is close to the original conductivity distribution. Meanwhile, as the number of singular values increases, the effect of noise will be enhanced in reconstructed image. Figure 6(d) shows the reconstructed image in a noise-free MAT-MI system, in which we can use 30000 singular values for reconstruction. Without noise, the algorithm attains a good image quality in the reconstruction. We can get a clear comparison from figure 6(e). It shows the more singular value we use, the more details of the conductivity were reconstructed by the algorithm. But the noise effect will increase as we use more singular values. The truncation index must be therefore established taking into account the trade-off between noise reduction and details reconstruction of the conductivity distribution. The SNR line in figure 4 is a simple method to estimate the truncation index.

B. EXPERIMENT RESULTS

In addition to the numerical studies, we tested the feasibility of the algorithm proposed experimentally on a conductive silicone rubber phantom. The settings of the experiment have

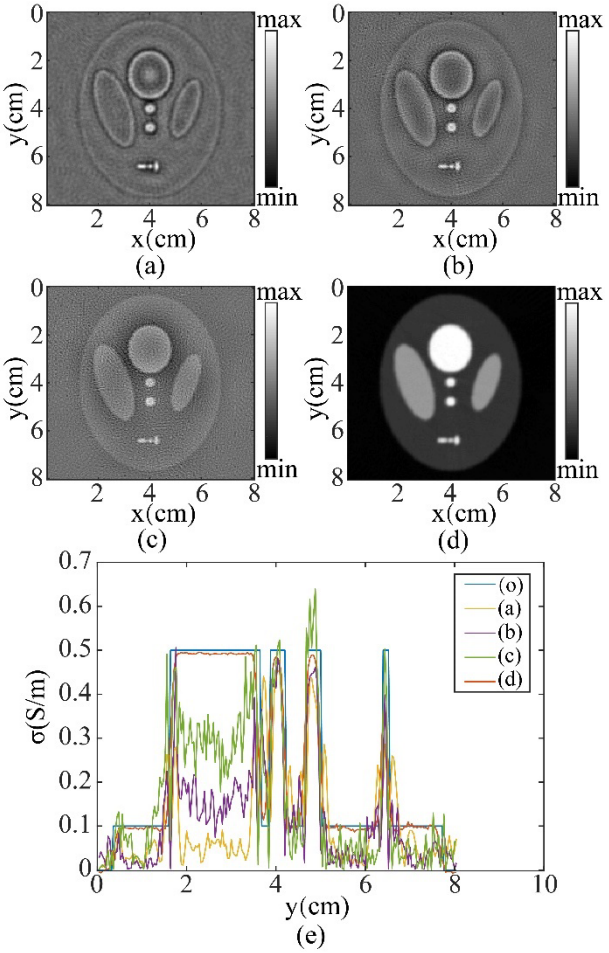

FIGURE 6. Original the influence to the reconstructed results by using different amounts of the singular values. (a) Reconstructed image using 5000 singular values with SNR = 20dB; (b) reconstructed image using 10000 singular values with SNR = 20dB; (c) reconstructed image using 15000 singular values with SNR = 20dB; (d) reconstructed image using 30000 singular values without noise; e) line graph of the conductivity distribution alone x = 4cm in figure (a) to (d), and (o) means the original distribution of the conductivity alone x = 4cm.

been mentioned in II-C section. Figure 7(a) shows the top view of the conductive silicone rubber phantom, the conductivity of the phantom is about 8000S/m. Figure 7(b) shows the measured acoustic signal when the scan angle is 90°. The results show that the induced acoustic signals come mainly from the boundaries where the conductivity changes obviously. By analyzing the SNR of the system, the SNR of the system is about 10dB. According to figure 4, about 10000 singular values can be used for reconstruction. In order to weaken the boundary effect, we use 15000 singular values for verifying the algorithm. Figures 7(c) and (d) show the reconstructed results by using 5000 singular values and 15000 singular values respectively. For the algorithm using 5000 singular values, the conductivity boundary of the phantom could be clearly imaged. When 15000 singular values are used in the proposed algorithm, the reconstructions provide a higher matching image to original conductivity distribution. As shown in figures 7(c) and (d), the more singular values we used for reconstruction, the more details will be presented.

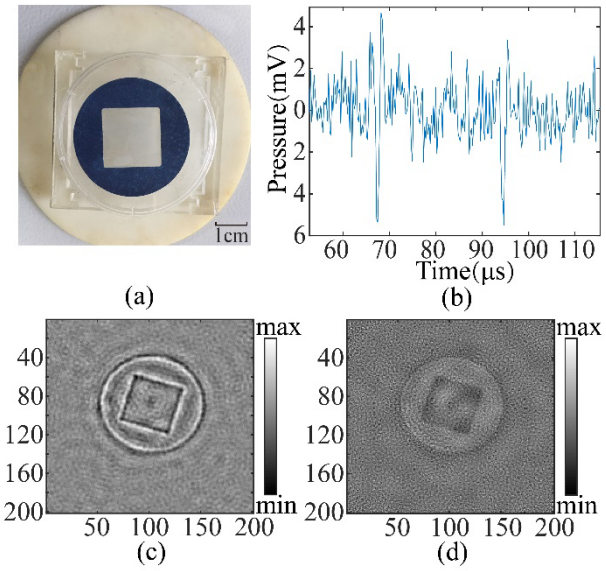

FIGURE 7. Experiment phantom, detected signals and the reconstruction results of the phantom conductivity. (a) Top view of the phantom; (b) temporal MAT-MI signal detected when the scan angle is 90°; (c) reconstructed conductivity distribution using 5000 singular values; (d) reconstructed conductivity distribution using 15000 singular values.

IV. DISCUSSION

In this paper, we built a system matrix of MAT-MI imaging system, and calculated the singular values. We proposed a TSVD based image reconstruction algorithm in which the desired information of the conductivity distribution was directly associated with the ultrasound signals. This approach is based on a discretization of the MAT-MI forward model, which is given by a linear integral equation. The kernel function of this equation establishes the ultrasound pressure induced by magneto-acoustic effect as a function of distribution of the conductivity. We assume that the ultrasound generation, propagation and acquisition are all performed in a 2-D region, so that a rectangular grid of points covering such region can be defined. Then the coupling of MAT-MI can be transformed to a numerical matrix, which contains all the information of MAT-MI experiment system. Because the system matrix was a linear system, so this method could be used for the conditions which were linear. For a different condition in the experiment, we could update the system matrix with the new conditions. Then we computed the singular values of the new system matrix. The matrix is independent of conductivity distribution and ultrasound pressure. In this method, the signals acquired by transducers at a set of positions and instants are expressed in a vector form. Since there is no change in the experiment conditions, the singular values can be computed once for a given MAT-MI framework. From the singular value decomposition, the relationship between SNR and the singular values of system matrix can be identified clearly.

The performance of the proposed algorithm was assessed by reconstructing simulated and experimental data. The review [19] presented back-projection algorithm and vector source method for the MAT-MI research. The bandwidth

limitation of ultrasound measurement was handled with inverse filtering and least square fitting over space in homogeneous regions, then the beamforming algorithm was applied for reconstruction. The inverse filtering of the ultrasound pressure signal was greatly affected by noise in our experiment, we couldn't get the ultrasound pressure signals with full bandwidth in current conditions. So, we chose back-projection algorithm for comparison, which was a classic reconstruction algorithm in MAT-MI. The result has clearly revealed that regularized the reconstruction algorithm based on TSVD have a clear advantage over back projection algorithm in terms of image quality when a MAT-MI system with a low SNR are considered. From figure 4, we can get the relationship between the SNR and the singular values. For current system, 3000-5000 singular values are enough to reconstruct the boundary of the conductivity distribution. Because most of the information of the MAT-MI signals came from the boundary of the conductivity distribution. The reconstruction process could be carried out with a SNR which is lower than 10dB for a boundary reconstruction. The influence of the number of singular values on the reconstructed results has also been studied in this paper. Therein it was found that the more singular values we used, the more details can be reconstructed. But due to the influence of the noise, a truncation index should be chosen for reconstruction. In our MAT-MI experiment system, there's a trade-off between the resolution of the reconstructed conductivity distribution and the noise level of the pressure. Through the system matrix algorithm, we can make maximum use of the information in ultrasound pressure signals by different noise level.

Although the system matrix algorithm shows a better reconstructed results for MAT-MI, there are still some drawbacks. One of the most important is the memory requirement. The system matrix and the singular value decomposition might consume a large amount of memory. In our MAT-MI reconstruction framework, about 65GB memory should be used in SVD computing and the matrix storing. Reducing this may limit the resolution and the accuracy of the reconstructed image. For the larger region of interest and smaller grids, the matrix compression scheme and the compressed sensing method could be applied. The approaches will be studied in future works. In the experiment study, the max electric pulse flowing in the circular coil is about 85A. The MAT-MI signals were very weak due to the output limitation of our excitation source. In order to get the efficient MAT-MI signal feature and use 15000 singular values for verifying the algorithm in this study, a signal-to-noise ratio of at least 20dB is required in the experiment. So we choose a phantom whose conductivity is about 8000s/m for improving the SNR of our experiment system. We will improve the magnetic stimulation device for applying this method to the biological tissue.

V. CONCLUSION

In conclusion, the analysis of the singular values can lead to an accurate inversion of MAT-MI, especially for a low SNR system, and can be applied in practical experiment systems. We expect that the TSVD based reconstruction algorithm proposed in this work will help to analyze the physical process and to obtain accurate high-resolution conductivity images for MAT-MI.

REFERENCES

[1] A. J. Surowiec, S. S. Stuchly, J. R. Barr, and A. Swarup, "Dielectric properties of breast carcinoma and the surrounding tissues," *IEEE Trans. Biomed. Eng.*, vol. BME-35, no. 4, pp. 257–263, Apr. 1988.

[2] K. R. Foster and H. P. Schwan, "Dielectric properties of tissues and biological materials: A critical review," *Crit. Rev. Biomed. Eng.*, vol. 17, no. 1, pp. 25–104, 1989.

[3] S. Gabriel, R. W. Lau, and C. Gabriel, "The dielectric properties of biological tissues: II. Measurements in the frequency range 10 hz to 20 GHz," *Phys. Med. Biol.*, vol. 41, no. 11, pp. 2251–2269, Nov. 1996.

[4] Y. Xu and B. He, "Magnetoacoustic tomography with magnetic induction (MAT-MI)," *Phys. Med. Biol.*, vol. 50, no. 21, pp. 5175–5187, Nov. 2005.

[5] R. Xia, X. Li, and B. He, "Reconstruction of vectorial acoustic sources in time-domain tomography," *IEEE Trans. Med. Imag.*, vol. 28, no. 5, pp. 669–675, May 2009.

[6] X. Sun, F. Zhang, Q. Ma, J. Tu, and D. Zhang, "Acoustic dipole radiation based conductivity image reconstruction for magnetoacoustic tomography with magnetic induction," *Appl. Phys. Lett.*, vol. 100, no. 2, Jan. 2012, Art. no. 024105.

[7] L. Mariappan and B. He, "Magnetoacoustic tomography with magnetic induction: Bioimepedance reconstruction through vector source imaging," *IEEE Trans. Med. Imag.*, vol. 32, no. 3, pp. 619–627, Mar. 2013.

[8] L. Mariappan, G. Hu, and B. He, "Magnetoacoustic tomography with magnetic induction for high-resolution bioimepedance imaging through vector source reconstruction under the static field of MRI magnet," *Med. Phys.*, vol. 41, no. 2, Jan. 2014, Art. no. 022902.

[9] W. Zhang, R. Ma, S. Zhang, T. Yin, and Z. Liu, "Image reconstruction in magnetoacoustic tomography with magnetic induction with variable sound speeds," *IEEE Trans. Biomed. Eng.*, vol. 63, no. 12, pp. 2585–2594, Dec. 2016.

[10] R. Ma, X. Zhou, S. Zhang, T. Yin, and Z. Liu, "A 3D reconstruction algorithm for magneto-acoustic tomography with magnetic induction based on ultrasound transducer characteristics," *Phys. Med. Biol.*, vol. 61, no. 24, pp. 8762–8778, Dec. 2016.

[11] J. Fessler, "Model-based image reconstruction for MRI," *IEEE Signal Process. Mag.*, vol. 27, no. 4, pp. 81–89, Jul. 2010.

[12] S. Boudabbous, D. Arditi, E. Paulin, A. Syrogiannopoulou, C. Becker, and X. Montet, "Model-based iterative reconstruction (MBIR) for the reduction of metal artifacts on CT," *Amer. J. Roentgenol.*, vol. 205, no. 2, pp. 380–385, Aug. 2015.

[13] A. Buehler, A. Rosenthal, T. Jetzfellner, A. Dima, D. Razansky, and V. Ntziachristos, "Model-based optoacoustic inversions with incomplete projection data," *Med. Phys.*, vol. 38, no. 3, pp. 1694–1704, Mar. 2011.

[14] X. L. Deán-Ben, R. Ma, A. Rosenthal, V. Ntziachristos, and D. Razansky, "Weighted model-based optoacoustic reconstruction in acoustic scattering media," *Phys. Med. Biol.*, vol. 58, no. 16, pp. 5555–5566, Aug. 2013.

[15] Q. Ma and B. He, "Magnetoacoustic tomography with magnetic induction: A rigorous theory," *IEEE Trans. Biomed. Eng.*, vol. 55, no. 2, pp. 813–816, Feb. 2008.

[16] H. Ammari, J. Garnier, H. Kang, L. H. Nguyen, and L. Seppecher, "Mathematics of super-resolution biomedical imaging," ETH Zürich, Zürich, Switzerland, Tech. Rep. 2016-31, 2016.

[17] C. D. Meyer, *Matrix Analysis and Applied Linear Algebra*. Philadelphia, PA, USA: SIAM, 2000.

[18] L. A. Shepp and B. F. Logan, "The Fourier reconstruction of a head section," *IEEE Trans. Nucl. Sci.*, vol. 21, no. 3, pp. 21–43, Jun. 1974.

[19] X. Li, K. Yu, and B. He, "Magnetoacoustic tomography with magnetic induction (MAT-MI) for imaging electrical conductivity of biological tissue: A tutorial review," *Phys. Med. Biol.*, vol. 61, no. 18, pp. R249–R270, Sep. 2016.

REN MA was born in Jilin City, China. He received the B.S. degree from the Department of Biomedical Engineering, Zhejiang University, Hangzhou, and the Ph.D. degree from the Peking Union Medical College, Beijing, China.

He is currently a Research Associate with the Institute of Biomedical Engineering, Chinese Academy of Medical Sciences and Peking Union Medical College. His current research interest includes theoretical simulation in electromagnetic functional imaging.

MING YANG was born in Beijing, China. He received the B.S. degree in biomedical engineering from Zhejiang University, Hangzhou, Zhejiang, in 2012. He is currently pursuing the M.S. degree with the Institute of Biomedical Engineering, Chinese Academy of Medical Sciences and Peking Union Medical College, Tianjin.

His research interest includes magneto-acoustic tomography with magnetic induction, magnetically mediated thermo-acoustic imaging, and bioelectric measurements.

SHUNQI ZHANG was born in Tianjin, China. He received the M.S. degree in optical engineering from Tianjin University, Tianjin, and the Ph.D. degree from the Peking Union Medical College, Beijing, China.

He is currently an Associate Professor with the Institute of Biomedical Engineering, Chinese Academy of Medical Sciences and Peking Union Medical College. His current research interests include weak signal detection and biomedical imaging methods.

XIAOQING ZHOU was born in Tianjin, China. She received the Ph.D. degree in optical engineering from Tianjin University, Tianjin, in 2014.

She is currently a Research Associate with the Institute of Biomedical Engineering, Chinese Academy of Medical Sciences and Peking Union Medical College. Her current research interests include medical electromagnetic imaging, tissue optical imaging, and medical signal processing methods.

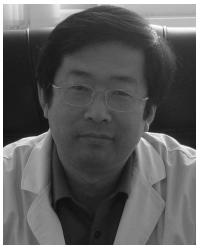

TAO YIN (Member, IEEE) was born in Shandong, China. He was graduated from Shandong University, Jinan. He received the M.S. degree from the Peking Union Medical College, Beijing, China.

He is currently a Full Professor with the Institute of Biomedical Engineering, Chinese Academy of Medical Sciences and Peking Union Medical College. His research interests mainly focus on neural electromagnetic stimulation and medical applications of electromagnetics. He is a member of the IEEE EMBS.

ZHIPENG LIU (Member, IEEE) was born in Shandong, China. She was graduated from Zhejiang University, Hangzhou. She received the Ph.D. degree from the Peking Union Medical College, Beijing, China.

She is currently a Full Professor with the Institute of Biomedical Engineering, Chinese Academy of Medical Sciences and Peking Union Medical College. Her research interests mainly focus on electromagnetic functional imaging and neural electromagnetic stimulation. She is a member of the IEEE EMBS.